10th International Conference on Fracture Mechanics of Concrete and Concrete Structures
FraMCoS-X
G. Pijaudier-Cabot, P. Grassl and C. La Borderie (Eds)
https://doi.org/10.21012/FC10.235482

MECHANICAL MODEL OF ROUGHENED CONCRETE OF EXISTING MEMBERS FOR SHEAR FAILURE MODE

Y. KATAGIRI[*], Y. TAKASE[†1], T. ABE[†2], K. SAKAMOTO[†3], T. HIWATASHI[†4] AND K. KATORI[†5]

[*] Graduate student, Division of Sustainable and Environmental Engineering,
Muroran Institute of Technology
Hokkaido, Japan
e-mail: 18041017@mmm.muroran-it.ac.jp

[†1] Associate professor, College of Environmental Technology, Muroran Institute of Technology
Hokkaido, Japan
e-mail: y.takase@mmm.muroran-it.ac.jp

[†2] Chief, Seismic Solution Department, TOBISHIMA Corporation
Tokyo, Japan
e-mail: Takahide_Abe@tobishima.co.jp

[†3] Chief, Seismic Solution Department, TOBISHIMA Corporation
Tokyo, Japan
e-mail: Keita_Sakamoto@tobishima.co.jp

[†4] Senior Researcher, Research and Develop Center, TOA CORPORATION
Tokyo, Japan
e-mail: t_hiwatashi@toa-const.co.jp

[†5] Professor, Dept. of Architecture, Fac. Of Sci. & Eng., Toyo University
Tokyo, Japan
e-mail: katori@toyonet.toyo.ac.jp

Key words: Seismic Retrofitting, Concrete Roughening, Shear Failure

Abstract: When buildings are seismically retrofitted, new members are connected to existing ones through a roughened concrete surface, which is constructed using a vibration drill. However, there are few studies on such roughened concrete surfaces. When the roughened concrete area ratio is small, supported failure occurs, while when the roughened concrete area ratio is large, shear failure occurs. In the case of support failure, the authors constructed a model that considers the microscopic roughness of the concrete surface. However, the shear failure has not been modeled yet. Therefore, in this study, additional experiments were conducted by constructing a mechanical model for shear failure. The maximum shear stress of the specimen could be calculated by considering the maximum shear stress level, according to Mohr's stress circle, and the roughened concrete area ratio after loading. Furthermore, the mechanical model for shear failure was constructed by using the maximum shear stress and the Hordijk model. Finally, it was demonstrated that the shear stress can be accurately reproduced.

1 INTRODUCTION

When buildings undergo seismic retrofitting, strengthening members are connected to existing members by roughening the concrete surfaces (using a chipping technique) and applying post-installed anchors. On the roughened concrete surface, the shear stress is transferred by contact. However, the shape, including the area and depth of the roughened concrete, is dependent upon the technique used by the construction worker. There is no relevant legislation concerning the roughened concrete in joint design[1] because it is rather difficult to guarantee the consistency and precise shape of the roughened concrete.

It has been reported that when applying post-installed anchors, without roughened concrete, the optimal strength decreases. However, the optimal strength exceeds the designed benchmark when concrete roughening is applied. Therefore, a method for better estimation of the shear strength of roughened concrete is required. There have been proposals for models using roughened concrete and anchors[2], although, there are still few studies that discuss only roughened concrete in detail.

According to shear-loading tests conducted in this study, two failure modes have been confirmed. When the roughened concrete area ratio (the ratio of joint surface area to horizontal projection area) is 0.3 or less, support failure occurs, which is caused by damage along the vertical section of the local roughness of existing concrete. When it is 0.5 or more, shear failure occurs on both the existing and the new side, which fail together. In the case of support failure, the authors constructed a model that takes into consideration the microscopic roughness of the concrete surface[3],[4]. However, we had not yet modeled the shear failure.

In this study, we carried out the additional testing and constructed a constitutive model for shear failure by using measured data of the roughened shape.

2 OUTLINE OF TEST ON ROUGHENED CONCRETE SURFACE

2.1 Details of specimens and test parameter

Figure 1 shows the details of the specimens used for the shear-loading test. Table 1 and Table 2 show the test parameters and the concrete and grout material properties, respectively. For the shear-loading test, a rectangular specimen (440 mm × 460 mm × 200 mm) was used. After roughening a concrete area of 375 mm × 200 mm, grouting mortar was cast on the surface. The test parameters were the roughened concrete area ratio r_0, the roughened concrete depth, the concrete compressive strength F_c, and the axial force σ_0. The estimated r_0 was set to 0.5 and 0.75. The specimen parameters were prepared with different depths and target compression strength was set to 9, 18, 27, and 30 N/mm^2. In addition, for the specimen with r_0 =0.5, the axial force was 0.24 and 0.48 N/mm^2. The name of the test specimen is the number that relates to the area ratio. The symbols denoting depth are S: shallow, N: normal, and D: deep and the numbers representing concrete strength and axial force are 1:σ_0=0.48 and 2:σ_0=0.24 N/mm^2.

Image analysis was used as a method of managing the roughened concrete area ratio of the specimen. Before subjecting the concrete to roughening, the joint surface of the specimen was painted black. The concrete surface was roughened by chipping, using a vibration drill, and r_0 was calculated using the difference in brightness between the black painted part and

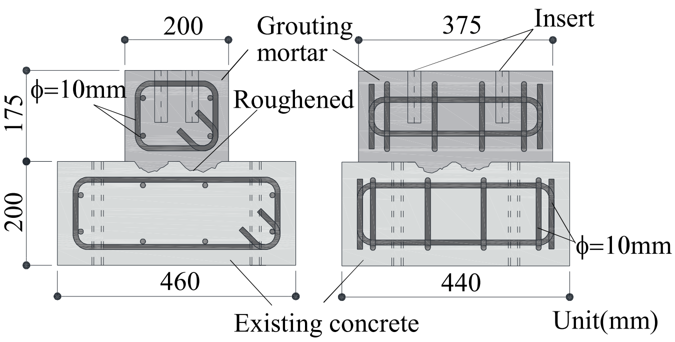

Figure 1 Details of specimen for shear loading test

Table 1 Test specimen parameters

Specimen	r_0	Measured area ratio	Axial force (N/mm^2)	Depth type
CH-50S-27-1	0.500	0.537	0.48	Shallow
CH-50N-9-1[5]		0.489	0.48	Normal
CH-50N-18-1[5]		0.499	0.48	Normal
CH-50N-27-1		0.477	0.48	Normal
CH-50N-27-2		0.499	0.24	Normal
CH-50N-30-1[5]		0.503	0.48	Normal
CH-50D-27-1		0.490	0.48	Deep
CH-75S-27-1	0.750	0.753	0.48	Shallow
CH-75N-18-1[5]		0.777	0.48	Normal
CH-75N-27-1		0.712	0.48	Normal
CH-75N-27-2		0.722	0.24	Normal
CH-75D-27-1		0.754	0.48	Deep
CH-100N-18-1[5]	1.000	−	0.48	Normal

r_0: Area ratio of roughening

Table 2 Material properties of concrete and grouting mortor

Specimen	Material	σ_B	E_c	σ_t
CH-50N-9-1[5]	Concrete	7.9	14.6	1.10
	Grouting mortor	72.3	24.4	4.10
CH-50N-18-1[5] CH-75N-18-1[5]	Concrete	17.1	24.7	1.83
	Grouting mortor	64.6	26.2	2.10
CH-50S,N,D-27-1 CH-75S,N,D-27-1	Concrete	26.9	26.1	1.85
	Grouting mortor	64.3	25.5	2.29
CH-50N-27-2 CH-75N-27-2	Concrete	26.1	16.1	1.83
	Grouting mortor	60.4	25.5	2.29
CH-100N-18-1[5]	Concrete	20.1	25.6	1.80
	Grouting mortor	72.3	24.4	4.10
CH-50N-30-1[5]	Concrete	31.7	30.1	2.50
	Grouting mortor	72.3	24.4	4.10

σ_B:Compressive strength(N/mm^2), E_c:Young's modulus (kN/mm^2) σ_t:Splitting strength(N/mm^2)

the concrete roughened part. Moreover, Table 1 shows the measured values of r_0 by image analysis, which demonstrates that roughening can be done using the area ratios as intended.

In addition, grease was applied to a smooth joint surface that was not subject to roughening, so that the influence of adhesion and frictional resistance, which occurred between the existing side concrete grout and the reinforced member side grout, was taken into consideration as much as possible.

2.2 Shape measurement of roughened

Photo 1 shows the 3D scanner, which was a non-contact and handy type. The three-dimensional shape data acquisition method was a pattern projection method. Radiated light from a 3D scanner was irradiated onto an object; three-dimensional data coordinates were acquired by analyzing the time difference and the irradiation angle at which the light was reflected. The specimen was fixed and measured while the 3D scanner was moved manually. Both the measurement intervals in the x- and y- directions were 0.1 mm, which was the minimum measurement interval of the 3D scanner used in this study.

2.3 Loading method of shear loading test

The equipment for the shear loading test is illustrated in Figure 2. Two 150 kN screw jacks, driven by the rotational power of the stepping

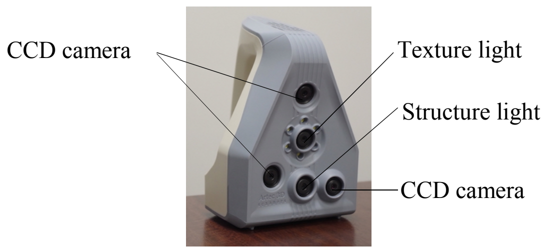

Photo 1 3D scanner

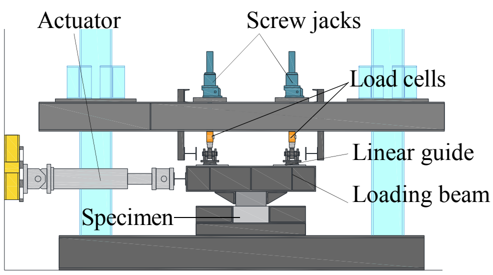

Figure 2 Equipment for shear loading test

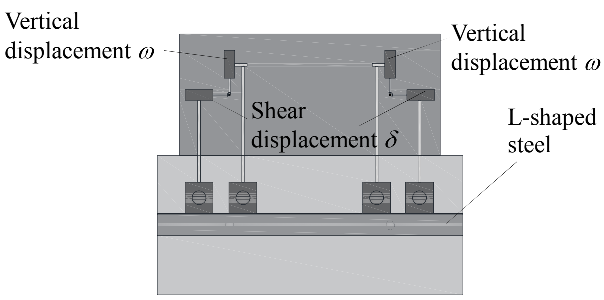

Figure 3 Measurement method of shear loading test

motor, were used in the shear loading test to control the axial force. A hydraulic actuator of 500 kN was used to control the horizontal load of the reversed cyclic loading. The displacement by the actuator in the shear direction was controlled manually. Regarding the axial force, the vertical jack was automatically controlled using the values of two displacement meters, which were measuring the vertical displacement. In addition, the two load cells were attached to the tip of the screw jack.

The measurement method is shown in Figure 3. L-shaped steel was connected to the concrete by bolts, and displacement meters were installed on the fixed L-shape steel. The vertical displacement ω and the relative shear displacement δ between the existing and strengthening members were measured.

3 RESULTS OF SHEAR LOADING TEST

3.1 Failure modes

When shear failure occurs, the existing side concrete and the new side grout fail simultaneously. Therefore, concrete and grout present shear failure in the same way. Photo 2 shows examples of roughened concrete surfaces. When comparing the area of roughened concrete, which is not painted black on the jointing surface, before and after loading, we notice that is increasing after loading. Thus, shear failure occurred in all specimens, and grout remains were seen in some places.

3.2 Comparison of test results

The test results of the τ–δ relations are shown in Figure 4. Table 3 shows the test results for maximum stress. The features of the τ–δ curve are: i) almost linear behavior up to the maximum stress, ii) sharp reduction of stress after the peak stress, and iii) constant stress after failure. Moreover, there was no significant difference in the maximum stress of the specimen due to differences in the roughened concrete's depth and axial force.

4 PROPOSED MODEL FOR SHEAR FAILURE

In this section, modeling is carried out assuming the tensile fracture acts on the roughened concrete surface for shear failure. The details are described below.

4.1 Maximum shear stress at shear failure of roughened concrete surface

Figure 5 shows the characteristics of the roughened shape after shear failure and the Mohr's stress circle acting on the roughened surface. Table 4 shows the area ratio of the specimen after loading. The shear failure does

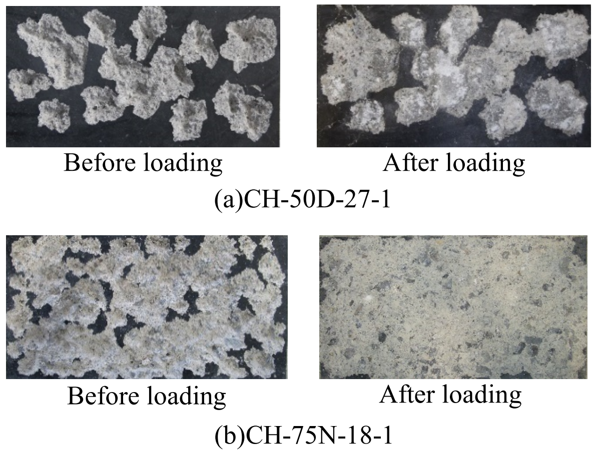

Photo 2 Examples of roughened concrete surface

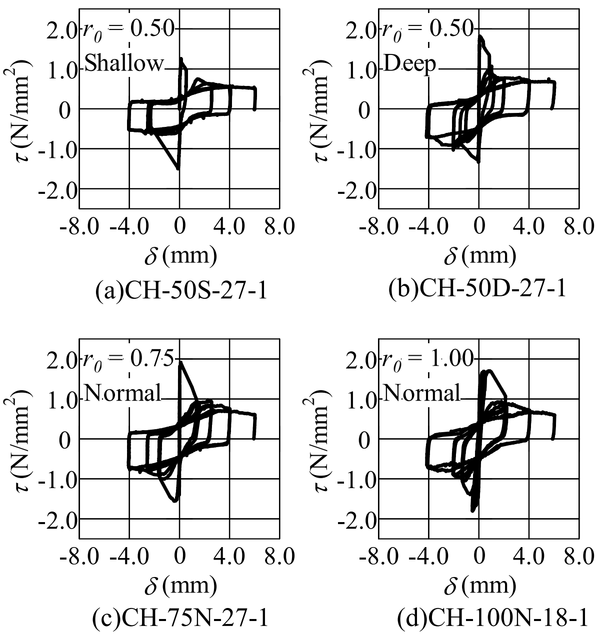

Figure 4 τ – δ relations

not fracture anything but the roughened concrete surface. A part where the smooth portion of the concrete remains as it is can also be seen in Table 4. The shear strength in the case where all shear surfaces fail is obtained from the Mohr's stress circle by the following equation:

$$\tau_{max} = \sigma_t + \sigma_0 \qquad (1)$$

where σ_t is the split strength and σ_0 is the axial force.

However, when obtaining the maximum stress τ_{max} for the shear failure of the roughened concrete surface, the roughened concrete area ratio ${}_{post}r_0$ after loading is used.

Furthermore, as not only concrete but also grout is fractured, the maximum shear stress τ_{max} is also expressed by the following equation, considering each split strength:

$$\tau_{max} = {}_{post}r_0 \cdot (\sigma_t' + \sigma_0) \qquad (2)$$

$$\sigma_t' = (\sigma_{tc} + \sigma_{tg})/2 \qquad (3)$$

where σ_{tc} is the split strength of concrete and σ_{tg} is the split strength of grout.

The area ratio after loading ${}_{post}r_0$ is averaged from the specimens of r_0=0.5 and r_0=0.75, Table 4.Table 4 shows the maximum shear stress calculated using Eq. (2). As compared with the test results, Table 3, a difference of about 0.05 ～0.73 N/mm^2 is observed. The reason for this is that shear failure is difficult to predict because failure occurs rapidly.

Table 3 Maximum shear stress of test results

Specimen	Shear displace ment δ (mm)	Maximum shear stress τ_{max} (N/mm^2)	Shear displace ment $-\delta$ (mm)	Maximum shear stress $-\tau_{max}$ (N/mm^2)
CH-50S-27-1	0.13	1.26	-0.12	-1.50
CH-50N-9-1[5]	0.73	1.33	-0.47	-1.43
CH-50N-18-1[5]	0.43	1.69	-0.48	-1.20
CH-50N-27-1	0.10	1.97	-0.03	-1.37
CH-50N-27-2	0.04	1.92	-0.04	-1.87
CH-50N-30-1[5]	0.24	1.81	-0.24	-1.61
CH-50D-27-1	0.07	1.82	-0.04	-1.33
CH-75S-27-1	0.09	2.09	-0.04	-1.34
CH-75N-18-1[5]	0.47	1.66	-1.64	-1.64
CH-75N-27-1	0.09	1.92	-0.44	-1.55
CH-75N-27-2	0.14	1.84	-0.01	-1.86
CH-75D-27-1	0.11	1.66	-0.02	-1.60
CH-100N-18-1[5]	0.78	1.70	-0.51	-1.80

4.2 Application of Hordijk model

Figure 6 shows an example of the tensile fracture phenomenon and constituent model of the concrete surface. It is considered that tensile fracture occurs locally at the same time as shear failure surface is formed. Therefore, in this study, a model was created describing the softening behavior, after the peak is constructed based on the Hordijk model[6], which is a constitutive law of concrete subjected to tensile stress. The Hordijk model equation is described as follows:

$$\frac{\tau}{\tau_{max}} = \left(1 + \left(3\frac{\delta}{\delta_u}\right)^3\right) exp\left(-6.93\frac{\delta}{\delta_u}\right) - \frac{\delta}{\delta_u}(1+3^3)exp(-6.93) \qquad (4)$$

where δ is the shear displacement and δ_u is the critical shear displacement.

4.3 Model for shear failure

When constructing the mechanical behavior for shear failure, as with the past model, using the previously calculated maximum shear stress τ_{max}, the peak is reached linearly. The mechanical behavior of the roughened concrete surface after the peak will be subject to the

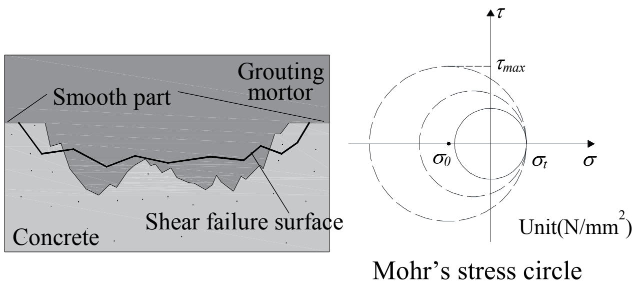

Figure 5 The characteristics of the roughened shape after failure and the Mohr's stress circle

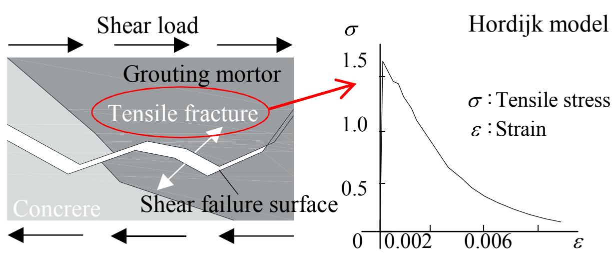

Figure 6 Example of the tensile fracture phenomenon and constituent model of the

Hordijk model. However, in this study, we set δ_u =10 mm in order to fit the critical shear displacement δ_u to the experimental values. In addition, for the constant stress behavior after the brittle fracture behavior, a model is constructed using the value of 1/3 of the maximum stress calculated in Section 4.1.

Table 4 Maximum shear stress and area ratio of roughening after loading

Specimen	τ_{max} (N/mm^2)	$_{post}r_0$	
CH-50S-27-1	1.71	0.706	
CH-50N-9-1[5]	2.06	0.798	
CH-50N-18-1[5]	1.64	0.789	
CH-50N-27-1	1.71	0.595	
CH-50N-27-2	1.54	0.603	
CH-50N-30-1[5]	2.53	0.649	Average
CH-50D-27-1	1.71	0.553	0.670
CH-75S-27-1	2.28	0.855	
CH-75N-18-1[5]	2.19	0.963	
CH-75N-27-1	2.28	0.884	
CH-75N-27-2	2.06	0.905	Average
CH-75D-27-1	2.28	0.873	0.896
CH-100N-18-1[5]	2.28	–	

5 COMPARISON OF TEST RESULTS AND PROPOSED MODEL

Figure 7 shows the results of the shear loading tests and the results of the proposed model. This experiment has reversed cyclic loading, however, the envelope curve on the positive side is used as the initial stage of the study. In specimen CH-75N-27-2, although the softening behavior after the peak can be well reproduced, the experimental value is overestimated by approximately 40% in the area where the stress is constant. It can be seen that CH-75S-27-1 does not follow the softening behavior after the stress peak. In the case of CH-50D-27-1, and CH-75N-27-1, the experimental values can be reproduced almost accurately.

Moreover, in the specimens of last year[5], the stress constant part can be generally reproduced. However, in specimens other than CH-50N-18-1, the softening behavior after the peak and the maximum stress cannot be evaluated. The reason for this may be that the load and displacement in the axial direction were more precisely controlled by the automatic control in this year's experiment. However, further experiments should be conducted to accumulate the necessary data.

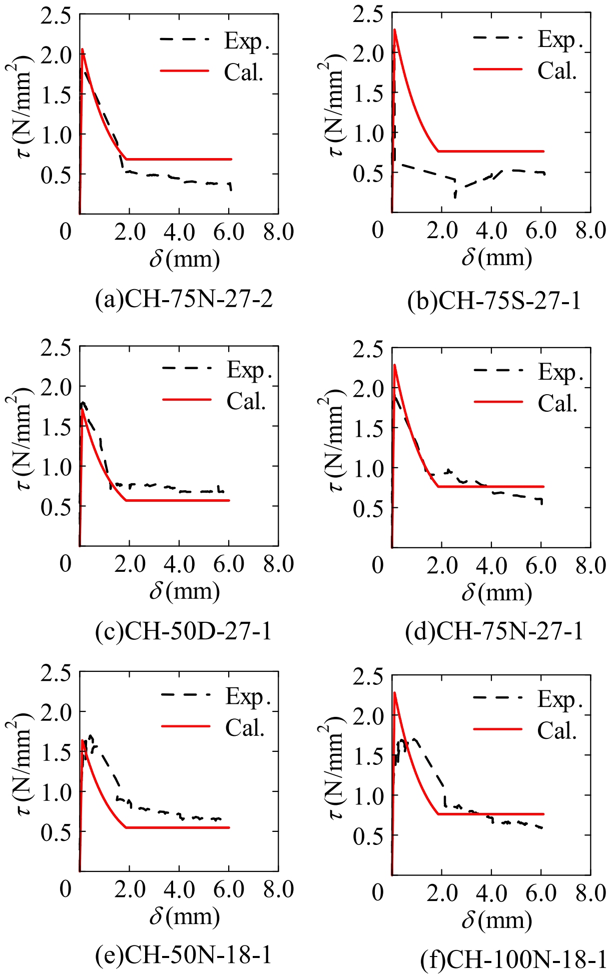

Figure 7 Comparison of test results and proposed model

6 CONCLUSIONS

The authors conducted shear-loading tests on specimens, which led to shear failure on the roughened concrete of joint surface, and based on the results, constructed a mechanical model for shear failure. The findings are listed below.

(1) Shear failure shows linear behavior up to its peak and brittle fracture behavior after its peak. Constant stress behavior was observed in all specimens.

(2) The maximum shear stress of the specimen could be calculated by considering the

maximum shear stress level of the Mohr's stress circle and the roughened concrete area ratio after loading.

(3) By using the maximum shear stress and the Hordijk model, a mechanical model for shear failure was constructed. Compared with the test results, the model was able to reproduce the phenomenon generally well.

The authors plan to advance future research so that experimental values can be reproduced with higher accuracy.

REFERENCES

[1] The Japanese Building Disaster Prevention Association: Seismic evaluation and retrofit,2017.7(in Japanese)

[2] Takase Yuya et.al.: Discussion on Mechanical Behavior of Joints Using Post-installed Anchor and Concrete Surface Roughening for Seismic Retrofitting, Proceedings of Compurational Modeling of Concrete Structures, pp.837-846,2014.3

[3] Isozaki Tsubasa et.al.:Shear stress transfer of roughened concrete for existing R/C members and mechanical model based on contact stress on local surface, J.Struct. Constr. Eng.,AIJ,Vol.83 No.750,1151-1159,2018.8

[4] Isozaki Tsubasa et.al.: Mechanical Model of Shear Stress Transfer of Roughened Concrete Surface for R/C Existing Member, Proceedings of Compurational Modeling of Concrete Structures, pp.973-982,2014.3

[5] Katagiri Yuki et.al.: Estimation of shear failure strength of roughened concrete surface using equivalent fracture surface depth, Proceedings of the Japan Concrete Institute,Vol.40,No.2, pp.967-972,2018.6

[6] D.A.Hordijk : Tensile and tensile fatigue behaviour of concrete; Experiments, modelling and analyses, HERON, Vol.37, No.1, pp.3-79, 1992